

Research article

Development of a new composite surface tensiometry parameter for quality evaluation of the maturation process of peloids by contact angle method

Davide Rossi ^{1*} and Nicola Realdon ²

Citation: Rossi D., Realdon N. - Development of a new composite surface tensiometry parameter for quality evaluation of the maturation process of peloids by contact angle method

Balneo and PRM Research Journal 2024, 15(4): 764

Academic Editor(s):
Constantin Munteanu

Reviewer Officer:
Viorela Bembea

Production Officer:
Camil Filimon

Received: 29.11.2024
Published: 23.12.2024

Reviewers:
Mihai Hoteteu
Iliescu Madalina

Publisher's Note: Balneo and PRM Research Journal stays neutral with regard to jurisdictional claims in published maps and institutional affiliations.



Copyright: © 2023 by the authors. Submitted for possible open-access publication under the terms and conditions of the Creative Commons Attribution (CC BY) license (<https://creativecommons.org/licenses/by/4.0/>).

- 1 Department of Pharmaceutical and Pharmacological Sciences, University of Padova, Via Marzolo 5, 35121 Padova, Italy
- 2 Department of Diagnostics and Public Health, University of Verona, Piazzale L.A.Scuro 10, 37134 Verona, Italy

* Correspondence: Davide Rossi, davide.rossi@unipd.it

Abstract: With the introduction of the rheological and surface tensiometry approaches, peloids started to be viewed as a geological complex system that needed to be characterized in an integrated way. The development of the Rossi factor revealed variations in the surface free energy of Euganean thermal muds as a function of their quality, conformity, and maturation degree. The Rossi factor consents to measuring the contact angle of Fomblin HC/25®PFPE Polyperfluoromethylisopropyl Ether by static sessile drop method. The development of the Kinetic Contact Angle sessile drop methodology, applied to the measurement of Fomblin HC/25® PFPE contact angles over time, led to the determination of an integrated surface tensiometry parameter for the evaluation of the maturation process of Euganean thermal peloids, here called the Maturation Mud Index. The Mud Maturation Index is based on the contact angle measurements performed onto peloids surfaces collected by Osservatorio Termale Permanente of University of Padova from 2005 to 2010. The Mud Maturation Index has shown a connection to the activity of thermal spas during their pelotherapy season. As a result, this index can serve as a valuable tool for surface tensiometry in assessing the maturation process quality of a peloid based on its level of maturation within the thermal activity of the Euganean Thermal Area in Padova, Italy.

Keywords: Polyperfluoromethylisopropyl Ether; peloid; contact angle, Maturation Mud Index, Euganean Thermal Area, surface tensiometry, Rossi factor

1. Introduction

The contact angle (CA; deg) that a liquid drop forms with a solid surface is an important measure of the wettability of a substrate. Measurements of the CAs in many research and industrial laboratories are among the most used ways to characterize the surfaces. The most often used technique for the CAs measurements is the sessile drop technique [1, 2]. Their widespread use is due to their simplicity and the small amount of liquid and surfaces needed [3]. The static contact angle methodology (SCA) is an important system parameter for many industrial and scientific processes in that it is a macroscopic manifestation of microscopic effects [4]. The primary motivation for measuring a CA is to assess the relative surface free energies (SFE; mJ/m²) of a complex system through the employment of many widely used conversion mathematical models [5-10, 1, 2].

The CAs and their measurements span every engineering field, from fluid dynamics to steel making and casting, microbial adhesion, mathematics, biomaterials, surface chemistry, pharmaceuticals, and geology [10, 11-17]. The method of Kinetic

Contact Angle (KCA) was recently defined to distinguish the terms of advancing and receding contact angle method (dynamic contact angle) from the measurements of CAs of a drop of a liquid left on a solid surface [18].

Recently, was introduced Polyperfluoromethylisopropyl Ether (PFPE) as a new kind of liquid test for the evaluation of solid and semi-solid complex systems surface tensiometry properties using SCA and KCA methodologies [17]. PFPE is a kind of liquid and polyfluoroalkyl substance (PFAS) [19].

The chemical family of per- and polyfluoroalkyl substances (PFAS) consists of three main groups: (a) Perfluoroalkyl acids (PFAAs) [19, 20], (b) Other PFAS, which include perfluoroalkanes, fluorinated aromatics, perfluoroalkyl ethers, and perfluoroalkylamines [21, 22], and (c) Polymeric PFAS. The polymeric PFAS can be further categorized into two types: perfluoropolyether (PFPE), such as Polyperfluoromethylisopropyl Ether, and fluoropolymers like polytetrafluoroethylene (PTFE) and polyvinylidene fluoride (PVDF) [23]. All PFAS are toxic except the PFPE, the only biocompatible PFAS [24] in commerce. The PFPE is biocompatible because of its hydrophobicity, lipophilicity and self-repellent properties due to the presence of a high amount of fluorine (~68%) that gives at the C-F bonds strong resistance, high stability and no chemical-physical reactivity [25]. The PFPE cannot induce acute toxicity, acute dermal toxicity, oral toxicity (no blood residues after 28 days), irritations at dermal/ocular level (as reported by CTFA safe testing guidelines), contact hypersensitivity, and it is not a comedogenic and mutagenic substance (Fomblin HC Classic: Dossier of toxicity test. Kalis Internal Report, Cornuda (Italy) September 2003).

Thanks to its biocompatibility, the PFPE (PFPEd) was considered a real liquid test for surface tensiometry evaluation of the quality of Euganean Thermal Muds (ETM) [16]. The PFPEd CAs measurement has been performed using the Rossi factor, a surface tensiometry parameter developed for the determination of the Surface Free Energy (SFE; mJ/m^2) of natural and artificial peloids avoiding friction forces and roughness factor at the liquid/peloid interface [13-16]. In the peloid sector, the PFPEd CA value is known as the TVS mud index® [13,15], and can be measured over time to evaluate the biological maturation process of a peloid.

The PFPEd CAs are related to the chemical and mineralogical properties of peloids [13, 15] and the hydrophobic, lipophobic, and self-repellent characteristics of Polyperfluoromethylisopropyl Ethers (ST; 18.1 mN/m , DC; 18.0 mN/m , PC; 0.1 mN/m). [25]. For this reason, the PFPEd CA was considered a surface tensiometry parameter that assesses the quality, conformity, maturation, and bioadhesive properties of the peloids. Thus, it also evaluates the mud's functional and therapeutic efficacy.

The aim of our work is the development of the Mud Maturation Index (MMI), a parameter capable of extrapolating qualitative information on the biological maturation process of Euganean thermal mud (ETM) from CAs of PFPEd [26, 27]. The objective of MMI is to provide a qualitative assessment of the maturation degree (MD) achieved by an ETM and to evaluate the management of the maturation process operated by a typical spa of the Euganean Thermal Area - ETA (Abano Terme and Montegrotto Terme – Italy). We propose the MMI as a quality parameter for the behaviour evaluation of the typical Spas Thermal Activity (STA) in use near the interested area. Figure 1 shows the typical seasonal behaviour of the N3 spa in May, June, and September.

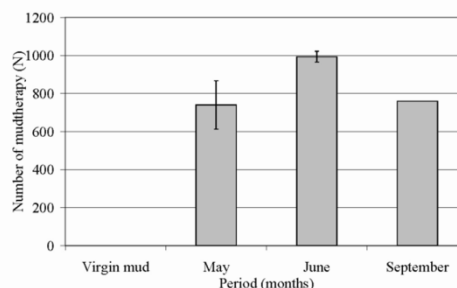


Figure 1

Based on the very widely used sessile drop method [1, 2, 28-39], the premise for the achievement of our objective was the application of KCA method at the measurements of PFPEd's CAs over the time. This method focuses on the use of PFPEd as a liquid test for static and over time CAs measurements (KCA) on surfaces of peloids.

This study was performed by the Department of Pharmacological and Pharmaceutical Sciences of the University of Padova (Italy) on surface tensiometry data of Euganean peloids collected in the period 2005-2010 by Osservatorio Termale Permanente - OTP (1996-2014) and sampled from the spas of Abano Terme and Montegrotto Terme (Padova) in collaboration with the Department of Geosciences of the same university.

2. Results

Generally, from a maturation process viewpoint, the months of June and July represent the period of maximum affluence of customs in this spa, while in September, the season is closing. In accord with the typical N3 thermal season shown in Figure 1, the month of May is viewed as the first phase of the maturation process, June the phase having the highest mud treatment activity of the season, and September the final phase of the maturation process.

Figure 2 shows the PFPEd CAs measured on the peloids sampled after three steps of maturation process (May, June and September).

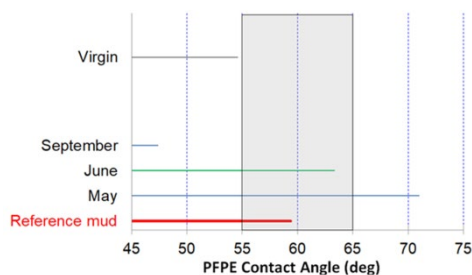


Figure 2

Figure 2 shows the high variability of the peloids' SFE over time. In particular, the virgin peloid (V) demonstrated an anomalously low level of PFPEd CAs, probably due to contamination of DC not derived from the maturation process.

By the pelotherapy season, the levels of PFPEd CAs decrease as DC increases and their link with the contact angles of PFPEd.

Figure 3 reports the Surface Tensiometry Profile (STP) of peloids sampled from the N3 spa in May, June, and September.

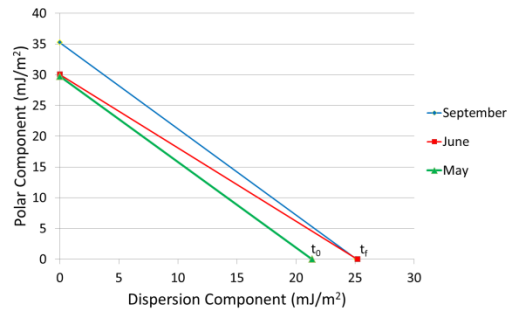


Figure 3

Figure 3 shows the variations in DC and PC during the maturation process of peloids used for pelotherapy from May to September.

2.1. Surface Tensiometry Maturation Parameter (STMP)

The DC present in a mature peloid originates from the organic compounds present in V (DC^B) and the organic compounds derived from the maturation process (DC^M) (Equation 2).

$$[2] DC^T (mJ/m^2) = DC^B (mJ/m^2) + DC^M (mJ/m^2)$$

Where DC^T is the total dispersion component present in a mature peloid, DC^B is the basal dispersion component due to the organic compounds present in V before the maturation process, and DC^M is the dispersion component derived from the biologic maturation process of peloid. Consequently, the SFE of a peloids derived from the contribution of DC^B and DC^M (Equations 3 and 4).

$$[3] SFE^T (mJ/m^2) = (DC^B + DC^M) + PC (mJ/m^2)$$

$$[4] DC^M (mJ/m^2) = DC^T - DC^B$$

Where SFE^T is the total surface free energy of a peloid, DC^B is the basal dispersion component due to the organic compounds present in the virgin peloid before the maturation process, and DC^M is the dispersion component derived from the biologic maturation process of peloid.

On these basis, we characterized the DC^M of a peloid using the variation of its DC over the time respect to PC (Equation 5).

$$[5] STMP = d(DC/PC) / dt.$$

Where STMP is Surface Tensiometry Maturation Process (STMP) parameter and $d(DC/PC)/dt$ is the variation of DC/PC ratio over the time.

Figure 4 illustrates the variation of the DC/PC ratio in relation to the maturation process within a number of pelotherapies performed during the seasonal operations of the N3 thermal spa. Based on these observations, a second parameter based on KCA methodology was developed to validate these findings.

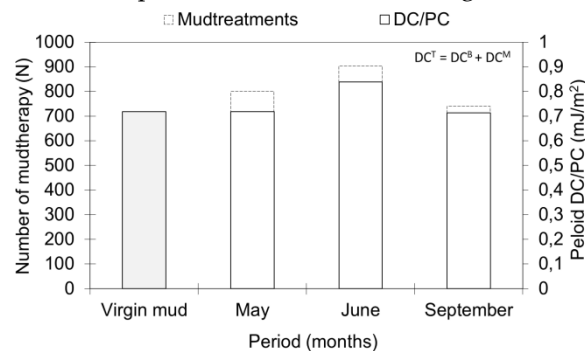


Figure 4

2.2. Surface Tensiometry Thermal Mud (STTM) parameter

To evaluate only the presence of DC^M , the PFPEd CAs were measured by KCA methodology to provide CAs over time. The behaviour of PFPEd CAs on the

surface of thermal muds was described mathematically by applying the power function $y = mx^b$. The power function allows us to avoid the logarithmic compression of the CAs data and increase the resolution between the single trend lines. In figure 5 are shown the behaviours of the line trends deriving from the measurements of CAs detected by the digital camera of the tensiometer for 10'' (225 cts).

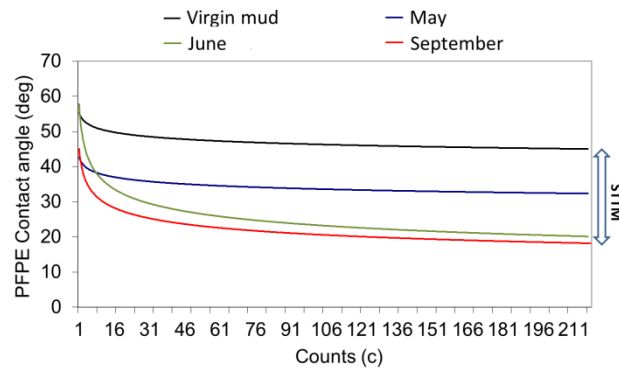


Figure 5

Figure 5 highlights that the PFPE CAs initially decrease and achieve over time a plateau for all the samples.

Furthermore, Figure 5 shows two different behaviours for each line trend corresponding to the interface area formed between PFPEd and the peloid surfaces. In particular, it is possible to recognize an initial and a final section. To extract more information about the dynamics of the maturation process, the behaviours of these two sections were identified and studied. Alternatively, at the measurement of the velocity of the droplet in mm/s [40], we associated the decrease of the PFPEd CAs with the increase of the peloid surface occupied (s) by the drop over the time (t). In this way, it was possible to calculate the speed (s/t) of the contact angle variations in function of the time (counts) in the two sections (1,31 and 31,61) of the trend lines (Equation 6 and 7).

$$[6] dv = ds/dc = dCA/dc$$

$$[7] dv = ds/dt = dCA/dt$$

Where dv is the variation of the PFPEd drop speed, ds is the variation of peloid surface occupied by PFPEd after the generation of peloid/PFPEd interface, dc is the increase of the counts, dCA is the variation of PFPEd CAs, dt is the variation of the time. It is possible to express the CA variations in area unit terms integrating the function [6] in the time (t) [8].

$$[8] A(c) = \int^{c_1} CA(c) dc = CA(c_1) - CA(c_0)$$

$$[9] A(t) = \int^{t_1} CA(t) dt = CA(t_1) - CA(t_0)$$

Where A is the area calculated between the power trend line and the x-axis in the range 1,61 counts, CA is the contact angle correspondent at the count c, dc is the count range 1,61 inside which the PFPEd drop spreads over the time t, and dt is the time range correspondent at count range 1,61.

According to these considerations, the difference between the V power trend line and the trend lines of the peloids with a higher degree of DC^M was called the STTM (Surface Tensiometry Thermal Mud) parameter.

The STTM can be calculated considering V as reference mud and the power trend lines corresponding at the CAs variations of other peloids samples collected in May, June and September (Equation 10).

$$[10] STTM = \int^{c_1} y^V(t) dt - \int^{c_1} y^n(t) dt$$

Where STTM is Surface Tensiometry Thermal Mud index expressed as the Area calculated between V and other peloid power trend lines, y is the y-axis value of each power trend line point corresponding at the PFPEd CAs measured in the range 1,61 counts, V is the virgin peloid, and n represents the other peloids samples (May, June, September).

Additionally, we considered the corresponding range of the correlation coefficient (R^2) presented in Table 1.

Table 1

Low b values correspond to low R^2 values into the range 0.60,0.70 and show that V and peloids collected in May have "low" levels of MD, while peloids collected in June ($b=-0.196$) and September ($b=-0.169$) show "high" MD. Figure 6 compares the b intercept from KCA and the CD/CP ratio calculated from SCA.

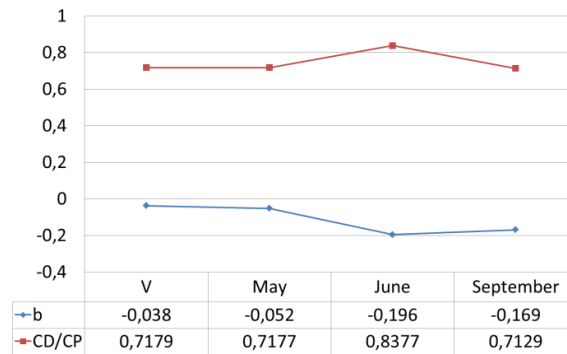


Figure 6

Figure 6 shows an inverse proportionality between SCA and KCA data that confirms the increase of DC^M in peloids collected from May to June. These data represent the natural increase of DC^M due to the development of biological activity over time.

However, STTM doesn't fully demonstrate its correlation with the difference in the number of pelotherapies performed in June and September. For this reason, we developed a third parameter derived from STTM called maturation process intensity (MPI).

2.3. Maturation Process Intensity (MPI) parameter

The MPI parameter can be obtained from the average PFPE spreading drop speed (SDS) measurements where the count (c) parameter was assumed as second (s) (Equations 10 and 11).

$$[11] \overline{SDS} = \bar{s}(c) \pm \delta$$

$$[12] \overline{SDS} = \overline{CA}(t) \pm \delta$$

Where \overline{SDS} is the average Spreading Drop Speed, \bar{s} is the average peloid surface occupied by PFPEd over the time after the generation of peloid/PFPEd interface, t is the PFPEd spreading drop time, \overline{CA} is the average contact angle measured over time, c is count, and δ is the standard deviations of s and CA s averages. We calculated the standard deviations (δ) of the data population next to the values points determined in the first (1,31) and second (31, 61) range for all the samples. Figure 7 puts the association of the δ values at the PFPEd SDS ($CA \cdot c - 1$) over time.

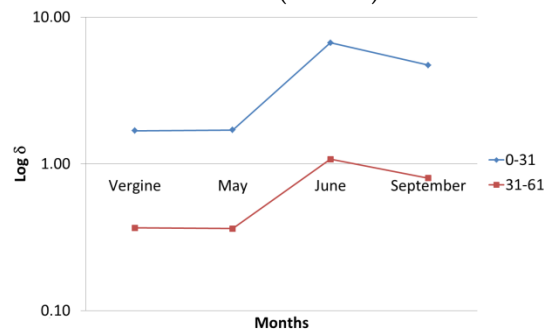


Figure 7

Figure 7 highlights the differential values between the CA variations speeds in the first (1,31) and in the second (31,61) section of the four power functions trend lines. Comparing the MPI levels of counts in ranges 1,31 and 31,61 for the standard

deviations d of both of them, Figure 7 shows that the highest differences in MPI values correspond at the month of June in accord with the number of pelotherapies performed during the N3 spa season, although the speeds registered in the final section (31,61) are lower than the others near the first section (1,31).

The MPI parameter corresponds at the different d of the PFPE drop speed variations observed between 0,30 and 30,60 counts (Figure 8).

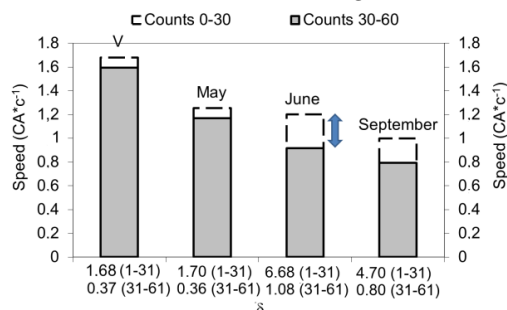


Figure 8

Figure 8 demonstrates that the highest differences in MPI values correspond to the month of June in accord with the number of pelotherapy performed during the N3 spa season.

To evaluate the MPI in peloids sampled from silos, we applied the SCA at the measurements of PFPEd CAs on samples collected from silos maturation plant S3, S5, S7, and ready-to-use thermal mud from pool maturation plant (BM) (Figure 9).

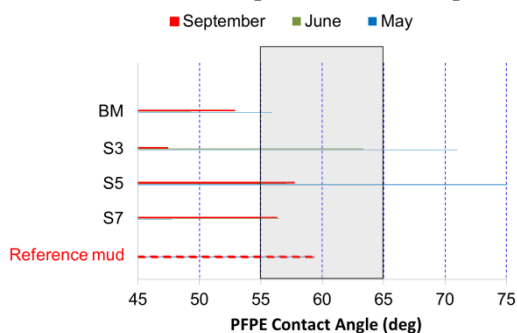


Figure 9

Figure 9 reveals a high variability of the surface free energy characteristics of the peloids found in the silos tested. In particular, the peloids sampled from silos 3 (S3) show a gradual decrease in the PFPEd CAs levels. By contrast, the peloid contain in silos 7 (S7) shows an increase of PFPEd CAs, and the peloid from silos 5 (S5) shows a break from June to September. The PFPEd CAs of sample BM decrease from May to June and increase from June to September as shown in Figures 8, 7, 2, and 1.

To define the real influence of the seasonal activity on the maturation process into N3 silos plants, we determined the MPI for peloids sampled in June (figure 10).

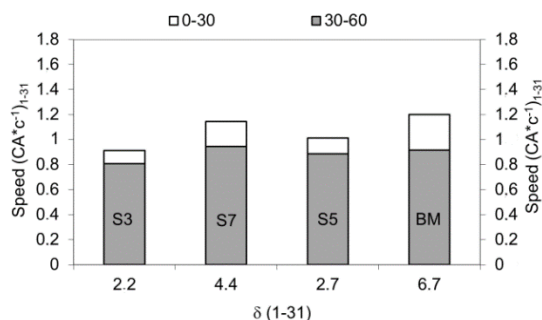


Figure 10

Figure 10 demonstrates less MPI values for silos 3 and 5 and more high values for silos N3 and BM. MPI monitors the variation of MD over time, and consequently, the peloid achieves its MD at the moment of the sampling from the maturation plant (June). In particular, Figure 10 shows that the better level of MPI is attributable to the peloid collected from the BM pool in June because of the higher presence of products from the biological maturation process. This appears in Figure 4 because the PFPEd drop speed variability decreases from May to June. The major MPI of the BM peloid corresponds to the increase of the DC^M present in the ready-to-use peloid in June because of the high maturation activity operated by the algal flora shown in Figures 8, 7, 6, 2, and 1.

Figure 11 shows a comparison between the standard deviations of PFPEd drop speed measured on peloids collected from the N3 spa.

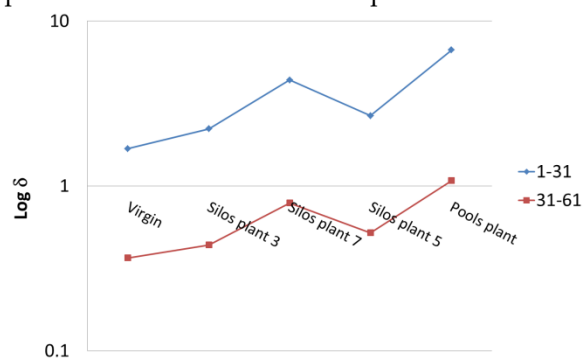


Figure 11

Figure 11 reveals that it was possible to determine the MPI parameter of peloids collected from different maturation plants in the spa in June.

In the end, Figure 12 reports the comparison between the d of average PFPE CAs in the range 1,61 counts and the STMP represented by the ratio DC/PC .

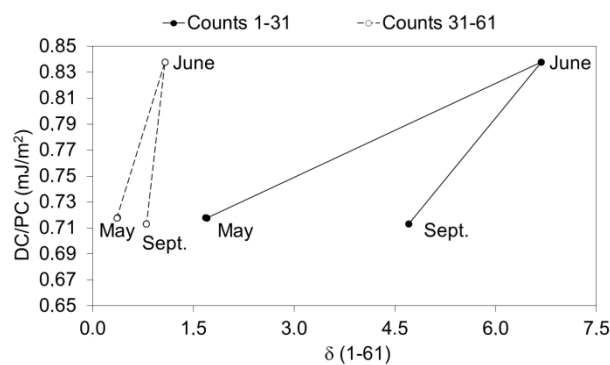


Figure 12

Figure 12 demonstrates the relationship between the DC^M and the intensity of the maturation process expressed by the MPI parameter.

2.4. Mud Maturation Index (MMI)

On the basis of this evidence, correlation analyses between STMP, STTM, and MPI parameters have been performed to develop the Mud Maturation Index (MMI).

The correlation study focused on samples collected from silos and manual plants operating in the N3 spa during the month of June in accordance with Figures 12, 8, 7, 6, 4, 2, and 1. Figure 13 reports respectively the correlation degree between (a) DC/PC (STMP) and the variation (%) of PFPEd SDS measured over time and (b) DC/PC (STMP) and d of average PFPEd CAs (MPI) measured on peloids sampled from S3, S5, S7 and BM.

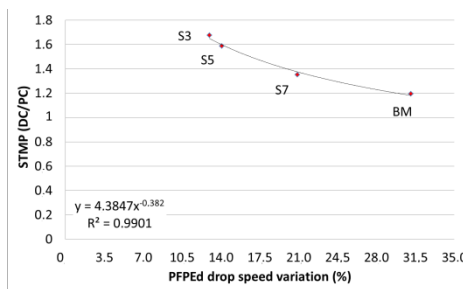


Figure 13a

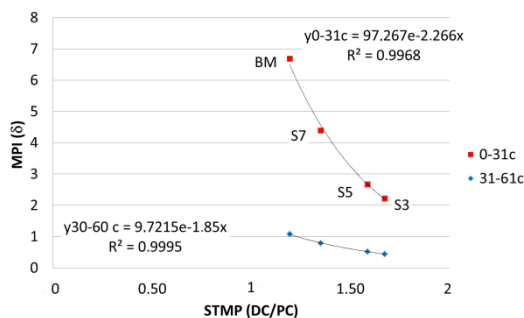


Figure 13b

Figure 13a shows that BM performs an intense peloid biological maturation activity while the STMP parameter indicates that a higher level of DC^M is in the peloids collected from silos plants. This is explainable by Figure 13b, which demonstrates that high MPI values correspond to peloids that don't reach the optimal maturation process step in June and vice versa by Figures 9 and 11. The exponential function shown in Figures 14a and 13b demonstrates the link between the increase of the DC^M deriving from the algal microflora resident and the decrease of PFPEd SDS variations. The high level of DC^M reached by the peloid corresponds to a decrease in MPI during the period considered (June). It thus becomes clear to see also the order in which the maturation process is performed in a typical S plant of a Euganean thermal spa.

In Figure 14, the analyses of the correlation between DC^M, linked at STMP index obtained from SCA methodology, and the parameter R², directly linked at STTM parameter obtained from KCA methodology, were extended at peloids sampled from different maturation process plants of N3 spa (BM and S3 plants) and those operating in other spas of Euganean Thermal Area such as N1 (plant BM2), N2 (plant BM5), HG (plant BM15), and AR (plant S2).

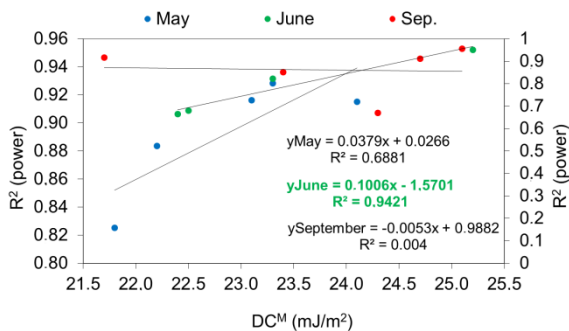


Figure 14

Figure 14 demonstrates that the MD of peloids inside an S plant can also be well represented by the degree of link between the DC^M product and the STTM parameter achieved over time. In accord with how discussed, it thus became to develop a new integrated surface tensiometry peloid index composed of STMP, obtained using the

SCA methodology, and MPI, obtained from STTM parameter calculated using KCA methodology, called here Mud Maturation Index (MMI) (Figure 15).

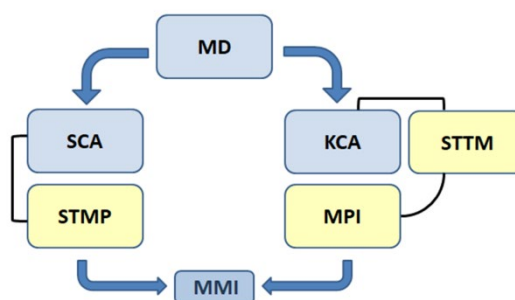


Figure 15

In the end, to allow us to assess the Spas Thermal Activity of N3 spa (STA^{N3}), we assumed as a dimensionless number the coefficient of correlation (R^2) of the linear functions used for the evaluation of the link degree between DC^M and the parameter R^2 , directly linked at STTM parameter (Figure 14).

Table 3 lists a comparison between thermal muds MD and STA^{N3} assessments for the silos plant of the N3 spa.

Table 3

Table 3 evidences the difference between the MD of each peloid sample and the STA achieved in each period considered by the plant. In the N3 case, the assessment associate at the MPI of the peloids becomes useful to give merit findings for the management of the maturation process operated by the spa personnel.

Accordingly with Tables 1, Table 3 show how the MD achieved by the peloids ready to use in June and September was “excellent”, while the STA in September result was “very low”. This fact is consistent with the low STA generally found at the end of the typical thermal season in use near the Euganean Thermal Area (see Figure 1).

3. Discussion

The levels of PFPEd CAs may be influenced by different factors, such as anomalous variations in the production of DC deriving from the maturation process, anomalies in the management of the regeneration process, or other variations due generally to chemical-mineralogical modifies of the mud system. As a consequence, the PFPEd CAs levels cannot so discriminate specifically the DC already present in V or from other external sources. The DC/PC ratio increased in June, primarily due to the increase in DC^M associated with biological maturation. This increase is particularly significant during June when the pelotherapies number is higher compared to May and September.

The introduction of PFPEd in the set of test liquids dim and gly, the measurement of PFPEd CAs using the Rossi factor (STMP parameter), the application of the KCA methodology and the application of the power function at the PFPEd CAs measured over time made up a new method for DC^M characterization. This method can be applied to any natural and artificial complex systems. In accordance with Figures 1, 3 and 4, Figure 5 highlights the differences in the amount of DC^T between V and the DC^M present in the peloids sampled in May, June and September.

The increase in the DC^M is due to the maturation process over the time reached in June, while in September, the maturation process ends one month. The trend line of V was assumed as a reference for the increase's evaluation of DC^M in the peloids.

In accordance with above observations, the STTM parameter was identified as a qualitative marker for surface tensiometry, specifically used for the evaluation of a peloid in the context of MD. Using the STTM parameter, we developed an assessment method for peloids, which is based on the intercept (b) value derived from the

trend lines generated by applying a power equation to the contact angle (CA) measurements over time (see Figure 5).

This assessment method revealed a link between the SDS differences shown in Figure 7 and the typical decrease of the first traits of the trend lines shown in Figure 5. In particular, V and the peloid sampled in May demonstrate the same initial decrease and SDS differences, while in the month of June, the result was higher than in other samples.

As regards the second parameter, the highest differences in MPI values measured in June, together with the intense activity of the thermal spa in June (Figure 1), induced us to hypothesize a strong role of the intensity of the maturation process in the behaviours of the trend lines reported in Figure 3.

Although the thermal mud collected in September presents a “very good” assessment of MD ($b=-0.169$, $R^2 = 0,95$) (Table 3), the month of June reveals the highest decrease ratio in drop speed variations (-24%) correspondent at an increase of MPI in accord with how reported in Figures 7, 2 and 1. This data highlighted the highest b intercept value ($b=-0.196$) of the power trend line extrapolated by the measurement of PFPEd CAs on the surface of the peloid over the time in June. The highest MPI values in June are linked to the improvement of the maturation process because the DC^M increased over time.

In June, MPI is due to the high removal activity of the BM peloid for pelotherapy which has a great volume of unmaturing peloid and is available for further biological activity. Proper automatic mixing of the peloids in silos promotes an increase of MPI and MD, with a reduction in PFPEd SDS.

The highest MPI in June was observed in BM because the manual management of the maturation process did not lead to a satisfactory MD (Figure 9) respect that observed in silos plants 3, 5, 7 in which the maturation process performs automatically. For this reason, the MPI reached by BM is higher than other plants.

As regards the third parameter, the month of June is characterized by high variability in the maturation process with respect to May and September due to the increase of the DC/PC ratio expressed by the STMP index in accordance with Figures 8, 7, 6, 4, 2, and 1.

In the end, we considered the STA^{N3} a reflex of MMI about the DC^M product during the maturation process.

4. Materials and Methods

Sampling was conducted by OTP on “ready to use” ETM from maturation process pool plants during the biological maturation process [26]. Samples were collected from silos (S) and manual (BM) maturation plants operating in N3 test spa near the ETA and carried out in triplicate. Specimens of thermal mud were placed inside 100 ml PE-HD containers equipped with double stopper and under stopper and stored in controlled conditions (4 °C) before analysis.

ETM's surface tensiometry measurements were performed by SCA sessile drop and KCA methodologies over the time [18].

In Table 4 are listed the comparison between the instrumental parameters for SCA and KCA sessile drop methods.

Table 4

All measurements were carried out by OTP directly on untreated peloids on a static tensiometer [13-16]. For the SFE determination of the thermal muds, Fomblin HC/25PFPE (Solvay Solexis, Milan, Italy), diiodomethane (Dim) (Merck, San Louis, USA) and glycerine (Gly) (A.C.R.A.F., Roma, Italy) reference standard liquids test were used.

Polyperfluoromethylisopropyl Ether is produced by Fuzhou Topda New Material Co., Ltd. in Fuzhou, China, under the commercial name PFPE C-250 (2021). Figure 16 shows the Fourier-transform infrared spectroscopy (FT/IR) results for PFPE C-250

and Fomblin HC/25 PFPE. This comparison demonstrates that both products contain the same PFPE molecule.

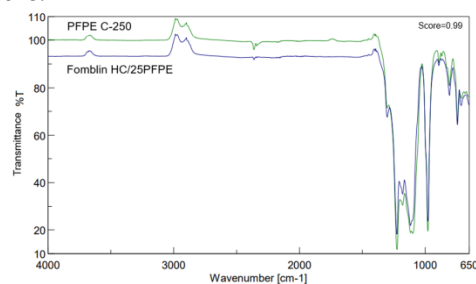


Figure 16

The CAs measurements performed by SCA (sessile drop method) lead to the evaluation of the SFE, dispersion component (DC; mJ/m^2), and Polar component (PC; mJ/m^2) by the Owens & Wendt model (Table 2) using DSA10 (Kruss, Hamburg, Germany) tensiometer software.

In particular, the PFPEd CA is measured using the Rossi factor [16, 17], a parameter based on a methodology capable of measuring the CA of hydrophobic, lipo-phobic and self-repellent liquids tests.

Table 2

The Rossi factor consents to the determination of the PFPEd CAs of different peloids in accordance with their chemical-mineralogical, texture, biological compositions, and spring water presence.

The peloid's maturation degree (MD) can be measured by determining its SFE, DC and PC. The SFE is the sum of its DC and PC (Equation 1).

$$[1] \text{ SFE } (\text{mJ}/\text{m}^2) = \text{DC } (\text{mJ}/\text{m}^2) + \text{PC } (\text{mJ}/\text{m}^2)$$

Where SFE is surface-free energy, DC is the Dispersion Component, and PC is the Polar Component. We analysed the changes in the SFE of "ready-to-use" peloids to verify the discriminating capability of this parameter during the maturation process.

5. Conclusions

Until today, the PFPEd CAs explained the link between the modification of surface free energy of peloid components during the maturation process over time and the variations of the PFPEd CAs measured by the SCA sessile drop method. The measurement of the PFPEd CAs variations shows for the first time the discriminating ability of surface tensiometry to distinguish the dispersion component (DC^M ; mJ/m^2) derived from the biological activity from the dispersion component due to the presence of other compounds (DC^B ; mJ/m^2). That allows us to determine the maturation degree (MD) and, consequently, the intensity of the maturation process achieved by a peloid at the sampling moment (MPI). Knowledge of the MD of a "mature" peloid than a virgin peloid (V) allows us to develop the Surface Tensiometry Thermal Mud (STTM), a new surface tensiometry parameter directly deriving from PFPEd CAs measured over time and, in particular, able to evaluate the maturation variations of a peloid. Given the typical *structure-surface* correlations that characterize every complex system [41], STTM and the Rheological Thermal Mud index (RTM) of a peloid are linked to each other [42]. The knowledge of the MD also allowed us to measure the entity of the STTM index of a peloid and consequently give a first surface tensiometry assessment of the maturation process quality reached by the peloid over time. The decrease in PFPEd SDS variations corresponds to improvements in the maturation process intensity (MPI) that is associated with the maturation degree (MD). MPI is essential for assessing the quality of spa thermal activity (STA) in relation to the dispersion component (DC^M), measured by the STMP parameter, during the biological maturation process. The set of STMP and MPI parameters constituted the Mud

Maturation Index (MMI), a composite parameter derived from the PFPEd CAs, linked to the RTM index, and specially developed for the evaluation of the maturation process quality of a peloid. Generally, the MMI opens possible perspectives for the quality of Spas Thermal Activity (STA) evaluation. The knowledge of the value of the activities of thermal spas could give the peloids a new qualification protocol directly linked to the customs index rating [13, 14, 17].

Author Contributions: Conceptualization, Davide Rossi; methodology, Davide Rossi; validation, Davide Rossi; formal analysis, Davide Rossi; investigation, Davide Rossi; resources; data curation, Nicola Realdon; writing—original draft preparation, Davide Rossi; writing—review and editing, Nicola Realdon; visualization, Nicola Realdon; supervision, Davide Rossi.

Funding: This research received no external funding

Institutional Review Board Statement: The study did not require ethical approval.

Informed Consent Statement: Not applicable

Data Availability Statement: Not applicable.

Acknowledgments: The authors would thank Kalis snc (Cornuda, Treviso, Italy) for its analytical support in the characterization of Fomblin HC/25® PFPE and PFPE C-250®.

Conflicts of Interest: The authors declare no conflict of interest.

References

1. Etzler, F. M. Characterization of Surface Free Energies and Surface Chemistry of Solids. In *Contact Angle, Wettability and Adhesion*, Ed.; Mittal, K.L. VSP, Utrecht, 2003; Volume., pp. 219–264.
2. Etzler, F. M. Determination of the Surface Free Energy of Solids. *Reviews of Adhesion and Adhesives* 2013, 1(1), 3–45. doi: 10.7569/RAA.2013.097301
3. Iliev, S., Pesheva, N. 2006 Nonaxisymmetric drop shape analysis and its application for determination. *J Colloid Interface Sci* 2006, 301, 677–684. doi:10.1016/j.jcis.2006.05.06.
4. Allen, J.S. 2003 An analytical solution for determination of small contact angles from sessile drops of arbitrary size. *J. Colloid Interface Sci* 2003, 261, 481–489. doi:10.1016/S0021-9797(03)00127-9.
5. Good, R.G., Girifalco, L.A. A theory for estimation of surface and interfacial energies. III. Estimation of surface energies of solids from contact angle data. *J Phys Chem* 1960, 64, 561–565.
6. Fowkes, M.F. Attractive forces at interface *Ind Eng Chem* 1964, 56, 40–52.
7. Owens, D.K. and Wendt, R.C. Estimation of the surface energy of polymers. *J App Polymer Sci.* 1969, 13, 1741–1747.
8. Wu, S. Calculation of interfacial tension in polymer systems. *J Polymer Sci* 1971, 34, 19–30.
9. Van Oss, C.J., Chaudhury, M.K. Good, R.J. 1988 Interfacial Lifshitz-van der Waals and polar interactions in macroscopic systems. *Chem Rev* 1988, 88, 927–941.
10. Van Oss, C.J., Giese, R.F. The hydrophilicity and hydrophobicity of clay minerals. *Clay Clay Miner* 1995, 43, 474–477.
11. Bettero, A., Marcazzan, M. © Semenzato, A. 1999 The quality of clays used for healing purposes. *Mineral Petrogr Acta* 1999, 152, 277–286.
12. Bettero, A., Dal Bosco, C., Rossi, D. © Veniale, F. 2005 Thermal mud evaluation by TVS model. In *Proceedings 3ème Col-loque du Groupe Français des Argiles*, Paris, France, 2005.
13. Veniale, F., Bettero, A., Jobstraibizer, P.G. Setti, M. Thermal muds: perspectives and innovations. *Appl Clay Sci* 2007, 36, 141–147. (doi : 10.1016/j.clay.2006.04.013)
14. Rossi D., Dal Bosco C., Jobstraibizer, P.G., Setti, M. Bettero, A. Thermal muds evaluation by tensiometric versus skin modeling (TVS modeling®). In *Proceedings 1º Congreso Iberoamericano de Peloides*, Vigo, Spain, 2007.
15. Rossi, D., Jobstraibizer, P.G., Dal Bosco, C., Bettero, A. A combined chemico-mineralogical and tensiometric approach for evaluation of Euganean Thermal Mud (ETM) quality. *J of Adh Sci Tech* 2012, 27 (1), 30–45. <https://doi.org/10.1080/01694243.2012.701501>

16. Rossi, D. The Quality Assessment of a Mudtherapy Protocol by Surface Tensiometry Using the Contact Angle Method: The Japanese Biofango® Therapy Experience. *Int Journ of Wettability Science and Technology* 2019, 1, 137–167.
17. Rossi, D. The Polyperfluoromethylisopropyl Ether used as a surface tensiometry tool for non-invasive quality assessment of peloids (TVS mud index®): An overview. *Balneo and PRM Research Journal* 2023, 14(4): 605.
18. Rossi, D., Rossi, S., Dobrzyński, D., Dolmella, A., Realdon, N. Assessment of spring waters from Lourdes (France) by contact angle method. *Surfaces and Interfaces*, 2020, 19, 100471. <https://doi.org/10.1016/j.surfin.2020.100471>.
19. Fenton, S.E., Ducatman, A., Boobis, A., DeWitt, J.C., Lau, C., Ng, C., Smith, J.S., Roberts, S.M. Human health toxicity of per- and polyfluoroalkyl substances. *Environmental Toxicology and Chemistry*, 2021, 40, 606–630.
20. Liu, W., Wu, J., He, W., Xu, F. A review on perfluoroalkyl acids studies: Environmental behaviors, toxic effects, and ecological and health risks. *Ecosystem Health and Sustainability* 2019, 5,(1), 1–19. <https://doi.org/10.1080/20964129.2018.155803>.
21. Tsai, W.T. Environmental hazards and health risk of common liquid perfluoro-n-alkanes, potent greenhouse gases. *Environment International* 2009, 35, 418–424.
22. Namazkar, S., Ragnarsdottir, O., Josefsson, A., Branzell, F., Abel, S., Abdallah, M. A. E., Benskin, J.P. *Environ Sci Processes Impacts* 2024, 26, 259–268.
23. European Environment Agency (2021), “Fluorinated polymers in a low carbon, circular and toxic-free economy”, Eionet Report - ETC/WMGE 2021/9.
24. Jellali, R., Jean-Luc Duval, J.L., Leclerc, E. Analysis of the biocompatibility of perfluoropolyether dimethacrylate network using an organotypic method. *Materials Science and Engineering* 2016, 65, 295–302.
25. Marchionni, G., Ajroldi, G., Pezzin, G. Molecular weight dependence of some rheological and thermal properties of perfluoropolyethers, *European Polymer Journal* 1988, 24 (12), 1211–1216.
26. Marcolongo, G., De Appolonia, F., Venzo, A., Berrie, C.P., Carofiglio, T., Ceschi Berrini, C. Diacylglycerolipids isolated from a thermophile cyanobacterium from the Euganean hot springs. *Natural Product Research* 2006, 20(8), 766–774.
27. Rossi, D. TVS® Mud Index: a rapid method for quality assessment of natural and artificial thermal muds. IDEASS, 2012. <http://www.ideassonline.org/innovations/brochureYellow.php?id=10http://www.ideassonline.org/public/pdf/BrochureTVS-ENG.pdf>
28. Lin, S.Y., Chang, H.C., Huang, P.Y. Measurements of dynamic/advancing/receding contact angle by video-enhanced sessile drop tensiometry. *Rev Sci Instrum* 1996, 67, 2852–2858.
29. Matsumura, H., Kawasaki, K., Kambara, M. Wetting of protein-adsorbed solid surfaces studied by a dynamic method. *Colloid Surface B* 1997, 8, 181–188.
30. De Meijer, M., Haemers, S., Cobben, W., Militz, H. Surface Energy Determinations of Wood: Comparison of Methods and Wood Species. *Langmuir* 2000, 16 (24), 9352–9359. doi: 10.1021/la001080n
31. Janocha B., Para G., Warszynski, P., Matheis, J., Adamczyk, Z. Combined measurement of dynamic surface-tension and dynamic contact-angles of surfactant solutions. *Bulletin of the polish academy of science. Chemistry* 2000, 48, 243–254.
32. Milchalsky, M.C. Saramago, B.J.V. Static and dynamic wetting behaviour of triglycerides on solid surfaces. *J Colloid Interf Sci* 2000, 227, 380–389.
33. Luner, P.E., Oh, E. Characterization of the surface free energy of cellulose ether films. *Colloid Surfaces A* 2001, 181, 31–48.
34. Stehr, M., Gardner, D.J. Walinder, M.E.P. Dynamic wettability of different machined wood surfaces. *J Adhesion* 2001, 76, 185–200.
35. Katelson, H.A., Meadows, D.L. Stone, R.P. Dynamic wettability properties of a soft lens hydrogel. *Colloid Surface B* 2005, 40, 1–9. doi: 10.1016/j.colsurb.2004.07.010
36. Wang, X.P., Chen, Z.F. Shen Z.Q. Dynamic behaviour of polymer surface and the time dependence of contact angle. *Sci China Ser B* 2005, 48, 553–559. doi: 10.1360/042004-22
37. Qiang, L., Hong, W., Xun, Z. Mingwei, L. Liquid droplet movement on horizontal surface with gradient surface energy. *Sci China Ser E* 2006, 49, 733–741. doi: 10.1007/s11431-006-2032-z
38. Shang, J., Flury, M., Harsh, J.B. Zollars, R.L. Comparison of different methods to measure contact angles of soil colloids. *J Colloid Interf Sci* article in press. doi:10.1016/j.jcis.2008.09.039

39. Chow, K.T., Chan, L.W. Heng, P.W.S. Characterization of spreadability of nonaqueous ethylcellulose gel matrices using dynamic contact angle. *J Pharm Sci-US* 2008, 97, 3467-3482. doi: 10.1002/jps.21227
40. Liao, Q., Wang, H., Zhu, X. Li, M. Liquid droplet movement on horizontal surface with gradient surface energy. *Sci China Ser E* 2006, 49, 733-741. doi: 10.1007/s11431-006-2032-z
41. Rossi, D., Lazzari, G., Franceschinis, E., Vettorato, E., Realdon, N. Characterization of Structure-Surface Correlations in Ointments Using Surface Tensiometry within the Concept of an Integrated Analytical Approach. *Langmuir* 2024, 40 (34), 18063-18070. doi: 10.1021/acs.langmuir.4c01613
42. Bettero, A. *Nuovi aspetti del termalismo*, Bologna, DSE Documentazione Scientifica Editrice, 1995.